NANO LETTERS

Letter

pubs.acs.org/NanoLett

PbSe Quantum Dot Solar Cells with More than 6% Efficiency Fabricated in Ambient Atmosphere

Jianbing Zhang,[†,∥] Jianbo Gao,[‡] Carena P. Church,[§,‡] Elisa M. Miller,[∥] Joseph M. Luther,[∥] Victor I. Klimov,[‡] and Matthew C. Beard*[,∥]

[∥]Center for Advanced Solar Photophysics, National Renewable Energy Laboratory, Golden, Colorado 80401, United States

[‡]Center for Advanced Solar Photophysics, Los Alamos National Laboratory, Los Alamos, New Mexico 87545, United States

[§]Department of Physics, University of California, Santa Cruz, California 95064, United States

[†]School of Optical and Electronic Information, Huazhong University of Science and Technology, Wuhan, Hubei 430074, China

Supporting Information

ABSTRACT: Colloidal quantum dots (QDs) are promising candidates for the next generation of photovoltaic (PV) technologies. Much of the progress in QD PVs is based on using PbS QDs, partly because they are stable under ambient conditions. There is considerable interest in extending this work to PbSe QDs, which have shown an enhanced photocurrent due to multiple exciton generation (MEG). One problem complicating such device-based studies is a poor stability of PbSe QDs toward exposure to ambient air. Here we develop a direct cation exchange synthesis to produce PbSe QDs with a large range of sizes and with in situ chloride and cadmium passivation. The synthesized QDs have excellent air stability, maintaining their photoluminescence quantum yield under ambient conditions for more than 30 days. Using these QDs, we fabricate high-performance solar cells without any protection and demonstrate a power conversion efficiency exceeding 6%, which is a current record for PbSe QD solar cells.

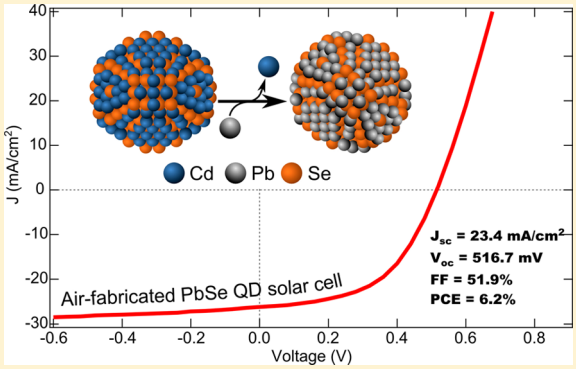

KEYWORDS: *Quantum Dots, Solar Energy Conversion, Cation exchange, Stability, PbSe*

Colloidal quantum dots (QDs) are among potential key players in the next generation of photovoltaic (PV) technologies.[1] They feature low-cost solution-phase processability,[2] large absorption cross sections, a spectrally tunable absorption onset (achieved via the quantum size effect),[3] and enhanced multiple exciton generation (MEG) or carrier multiplication (CM).[4−6] PbS QD based PVs (QD-PVs) fabricated under ambient atmosphere have recently demonstrated certified power conversion efficiencies approaching 9%,[7,8] a remarkable progress achieved just in a couple of years after the first report on a certified QD solar cell.[9,10] Among chalcogenide QDs, PbSe is an intriguing chemical system because of its unique and interesting properties. PbSe QDs exhibit highly quantum-confined excitonic states with confinement energies that can exceed 0.5 eV, which corresponds to band gap energies (E_g) in excess of 0.8 eV. The large degree of spatial confinement should induce a significant wave function leakage and therefore enhances electronic coupling between adjacent QDs that in turn should facilitate charge-carrier transport.[11] PbSe QDs have other properties favorable for the realization of practical PVs such as an easily scalable large batch synthesis, a narrow size distribution of resulting QD materials, and a fairly low density of intragap defects near commonly used metal-oxide window layers.[12]

Because of their excellent air stability, PbS QDs have been the focus of the majority of research efforts on QD-PVs. On the other hand, there is a significant interest in extending this work to PbSe QDs because of more efficient MEG than found in PbS QDs.[13,14] Specifically, the MEG-enhanced photocurrent so far has been only demonstrated in PbSe QD solar cells.[15,16] The studies of these devices, however, have been greatly complicated by the need for using inert environment during their fabrication, as even a very short exposure of PbSe QDs to ambient air results in their degradation. For instance, hydrazine-capped, *n*-channel PbSe QD field effect transistors (FETs) turn *p*-type after only 1 min of air exposure.[17] PbSe QD films treated with 1,2-ethane-dithiol (EDT) become heavily *p*-type upon exposure to oxygen.[18] Stability studies show that dispersions of PbSe QDs in hexane stored in air undergo rapid oxidation such that within a couple of hours 50% of the QD volume is transformed into oxidation products.[19] Thus, the efforts to explore MEG in practical devices can be greatly facilitated by the development of PbSe QDs that are both air-stable and allow for the realization of high-performance PVs.

Received: August 11, 2014
Published: September 9, 2014

   dx.doi.org/10.1021/nl503085v | *Nano Lett.* 2014, 14, 6010−6015

Researchers have explored several approaches for improving the stability of PbSe QDs. Most of them can be classified as attempts to passivate either under-coordinated Pb or under-coordinated Se sites.[20−22] Recently, chloride has been successfully employed to passivate Pb sites and thus prevent or slow down oxidation. Bae et al. found that exposing PbSe QDs to chlorine gas resulted in QD surfaces that were passivated with a thin $PbCl_2$ layer.[20] The use of $PbCl_2$ as a precursor resulted in PbSe QDs that were passivated in situ with $PbCl_2$.[23,24] Woo et al. recently studied NH_4Cl treated PbSe QDs and concluded that $PbCl_2$ forms an atomically thin halide layer on the (100) surfaces of PbSe that hinder oxidation.[25]

Various metal cations have been explored for passivating under-coordinated Se ions. This can improve the transport characteristics by reducing the number of deep electronic trap states.[26,27] Among various metals, cadmium has been the most effective and versatile, allowing for surface bonding both during the synthesis and in post-synthesis ligand exchange procedures.[26] Metal cations can be introduced post-synthesis via cation exchange reactions. Cation exchange is a powerful synthetic tool which finds many applications in the synthesis of novel nanostructures.[28] Using this technique, it is possible, for example, to extend synthetic methods developed for Cd-chalcogenides nanostructures with well-defined shapes, sizes, and compositions to Pb-chalcogenides.[29] As an example of this strategy, Luther et al. demonstrated a route for fabricating PbX nanorods starting with nanorods of CdX.[30] In the course of those studies, they found that it was difficult to promote the direct exchange of Cd^{2+} for Pb^{2+} due to the similarities in their valency, hardness, and electronegativity.[30] To resolve this issue, they applied a two-step protocol where Cd^{2+} was first exchanged for Cu^{+} and then Cu^{+} was replaced by Pb^{2+}. Cation exchange schemes, in which PbSe QDs are exposed to Cd-oleate to form a thin shell of CdSe, have been pursued to enhance QD stability.[31] The CdSe outer layer does improve environmental stability of the QDs, but it also produces an electronic barrier that impedes charge transport. In principle, one could optimize the amount of Cd within the treatment protocol in order to obtain favorable passivation without significantly hindering electronic transport as explored in recent studies.[32]

Here, we develop in situ chloride and cadmium passivation simultaneously through a cation exchange reaction that converts CdSe QDs directly into PbSe QDs without an intermediate step of Cd^{2+}-for-Cu^{+} exchange. We elucidate the nature of this passivation by high-resolution transmission electron microscopy (HRTEM), X-ray diffraction (XRD), and X-ray photoemission spectroscopy (XPS) and demonstrate that Cl and Cd ions reside on the PbSe QD surfaces. Furthermore, using PbSe QDs prepared in this manner we develop high-performance solar cells fabricated in ambient atmosphere. These PV cells show a power conversion efficiency exceeding 6%, which is a current record for PbSe-QD-based devices.

The ion-exchange process used here involves first synthesizing CdSe QDs of a desired size following previous reports.[33] The CdSe QDs are then injected into a hot $PbCl_2$/oleylamine (OLA) mixture. The $PbCl_2$/OLA mixture is an interesting system that has been previously explored for the direct synthesis of PbSe and PbS QDs.[24] Here we show that $PbCl_2$/OLA promotes direct cation exchange of Cd^{2+} for Pb^{2+} in a single reaction step. We developed the following protocol for this reaction: we first heat a mixture of $PbCl_2$ and OLA at 140 °C for 30 min. The resulting viscous solution is then set to a temperature ranging from 80 to 190 °C depending on the desired QD size (see below). Presynthesized CdSe QDs[33] (details are provided in the Supporting Information) are then rapidly injected followed by reduction of the bath temperature. The color of the solution changes immediately upon the injection of CdSe QDs, indicating that the cation exchange reaction proceeds very quickly.[34] Oleic acid (OA) is added to the reaction mixture to remove unreacted $PbCl_2$ and replace OLA ligands weakly bound to the QD surfaces.

In Figure 1, we plot the absorption spectra of PbSe QDs with mean diameters from 2.5 to 4.8 nm; the corresponding positions of the band-edge absorption peak are from 848 to 1486 nm. The line color in Figure 1 indicates from which CdSe sample the PbSe was made and the CdSe absorption spectra are displayed in Figure S1. Both the final size of the PbSe QDs and their size distribution depend upon the initial size and the size distribution of the CdSe QDs. (Figure S3 shows how the final PbSe QD size distribution depends on the initial CdSe size distribution). Furthermore, we verified that injection of CdSe QDs into a hot OLA without $PbCl_2$ does not cause the CdSe QDs to dissolve. Therefore, we conclude that the reaction does not proceed via dissolution of CdSe QDs followed by formation of PbSe QDs in the presence of Cd^{2+} but rather by direct cation exchange.[35] We also find that the cation-exchange reaction occurs for both wurtzite and zinc blende CdSe QDs (Figure S4).

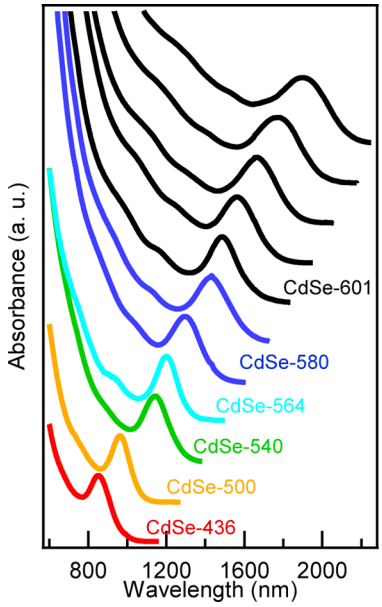

Figure 1. Absorption spectra of PbSe QDs synthesized by cation exchange from CdSe QDs. The wavelengths of the first exciton absorption peak of the initial CdSe QDs are noted for each PbSe QD spectrum. The samples with the wavelength of the band-edge transition greater than 1486 nm are synthesized using CdSe QDs with the 601 nm band-edge absorption feature as a starting material; see discussion in the text.

Larger sized PbSe QDs require a higher temperature reaction to ensure complete cation exchange (details for each reaction are reported in the Supporting Information). The kinetic and thermodynamic driving forces that result in favorable exchange reactions depend on many factors and elucidating general trends for guiding synthetic efforts is an active area of

dx.doi.org/10.1021/nl503085v | Nano Lett. 2014, 14, 6010−6015

nanoscience.[36,37] In thin bulk films, the solid-state diffusion of cations is the rate-limiting step and not the actual rate of cation exchange.[36] Therefore, a boundary between the two phases forms and the width of the boundary defines a reaction zone (location where the actual cation exchange takes place) which can be on the order of a few nanometers. The reaction zone is, among other factors, temperature-dependent. For cation exchange reactions that aim at converting the entire QD the zone width must be larger than the QD size as otherwise QDs may experience structural distortions. For example, when the temperature is not optimal for a given starting size of the CdSe QDs, ion exchange does not proceed to completion, and the nanoparticles coagulate (see Figure S5).

For sizes above ~5 nm, the required temperature is higher than 200 °C. The OLA/$PbCl_2$ solution, however, becomes unstable at such high temperatures. To resolve this problem we have developed a procedure for a post-ion-exchange growth of the QDs. As the cation exchange is performed at a relatively high temperature, continued growth of larger PbSe QDs via dissolution of smaller QDs can proceed if the temperature is maintained. In order to fabricate PbSe QDs with sizes greater than ~5.0 nm, we use 4.8 nm CdSe QDs as a starting material. We conduct Cd^{2+}-for Pb^{2+} exchange at T = 190 °C and then promote continued growth by introducing an additional amount of the selenium precursor (TOPSe) while maintaining the reaction temperature. The reaction conditions are chosen so that the additional growth occurs in the size-focusing regime.[24] Using this method, we have been able to extend the size range of PbSe QDs to ~6.3 nm; the corresponding absorption spectra are shown in Figure 1 by black traces.

The cation-exchange reaction presented here is performed at elevated temperatures where the thermal energy is sufficiently high to remove lattice stress and disorder that are typical for nanocrystals fabricated via room-temperature ion exchange.[36] This is confirmed by the HRTEM image in Figure 2a that does not display any apparent structural defect in the as-synthesized PbSe QDs. Figure 2b, which is the lower-resolution TEM images, shows that QDs are fairly monodisperse. We also compare the XRD patterns of the starting CdSe QDs to those of the final PbSe QDs and find no evidence of residual CdSe. XPS measurements (Figure S7) also find minimal residual Cd^{2+} (4% compared to Se for 2.9 nm PbSe QDs), and we do not observe evidence of significant Cd^{2+} in the UV−vis and photoluminescence (PL) spectra, which would manifest as broadened peaks, reduced PL QYs, or features associated with residual CdSe QDs. We conclude that CdSe QDs are fully converted to PbSe QDs in a direct cation exchange reaction.

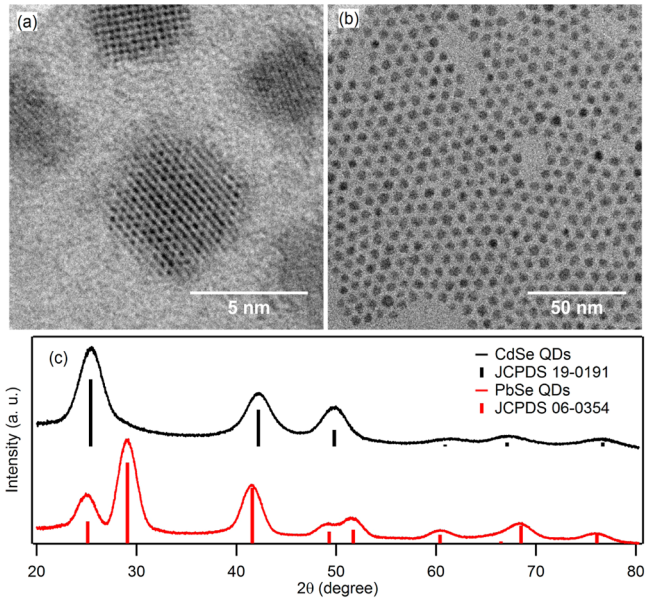

Figure 2. (a) HRTEM and (b) lower-resolution TEM images of resulting 4.7 nm PbSe QDs. (c) XRD patterns of 4.7 nm ion-exchanged PbSe QDs (red trace) and CdSe QDs (black trace) used as a starting material.

The stability of PbSe QDs can be characterized by tracking the position of the first exciton absorption peak and the PL quantum yield (QY) over time.[19] The absorption and PL data for two representative sizes are shown in Figure 3; panel a is for 2.9 nm QDs, and panel b is for 5.1 nm QDs. The PbSe QDs fabricated via cation exchange are stable in air when stored in hexane in contrast to QDs synthesized using PbO as a precursor (Figure S6).[38] The 2.9 nm PbSe QDs made via ion exchange show a PL QY of ~43% which remains constant for at least 30 days. Their stability is similar to that of noncation-exchanged PbSe QD fabricated using $PbCl_2$ as a precursor.[24] This suggests that the enhanced air-stability is governed by the chloride passivation but not the metal cation. In fact, the Cl:Pb ratio (determined via XPS; Figure S7) of ~3 nm PbSe QDs produced via the cation exchange is 0.44, which is similar to that for the $PbCl_2$ based syntheses.[23,24] The enhanced air-stability resulting from chloride termination is likely linked to the larger formation energy of $PbCl_2$ (−359 kJ/mol) compared to PbSe (−100 kJ/mol) or PbO (−219 kJ/mol).

In our samples, residual cadmium is not likely to reside in the interior of the PbSe QDs, as due to self-purification,[39] residual Cd is expelled to the QD surface. We have at least two pieces of evidence in support of this conclusion: (1) The amount of residual Cd is similar to that in previous reports in which Cd was used for post-synthesis surface treatments;[22,26] and (2) while being stable in hexane, ion-exchanged PbSe QDs undergo surface etching in a tetrachloroethylene (TCE) solution. Figure 3c displays the evolution of absorption spectra of the TCE solution of the 2.9 nm QDs during 30 days following their fabrication. A 50-nm blue shift of the first excitonic transition observed in these measurements is consistent with a ca. 0.2 nm shrinking of the QD diameter according to standard sizing curves. After 30 days of surface etching, the content of residual Cd decreases by 83% to values less than 1% with respect to Se implying that most of the Cd was lost as a result of surface etching. During the same time, the oxygen content increases by ~80%. Because PbSe QDs synthesized from $PbCl_2$ are stable in TCE,[24] we speculate that the blue shift observed for ion-exchanged samples results from Cd assisted surface etching. The loss of Cd during the etching and the apparent Cd-assisted character of this process support the assessment that Cd is located at the QD surface but not in the interior of the QD. Surprisingly, while affecting the position of the band-edge excitonic feature, surface etching does not lead to appreciable changes in the PL QY, as illustrated by the inset of Figure 3c.

We took advantage of the improved air stability of PbSe QDs fabricated via direct Cd^{2+}-for-Pb^{2+} cation exchange and used them to demonstrate high-performance solar cells fabricated under ambient conditions. We utilize a p−n junction device architecture that comprises ITO/TiO_2/PbSe QDs/MoO_3/Al; see device schematics in Figure 4a and a scanning electron microscopy (SEM) image in Figure 4b. The QD layer was

dx.doi.org/10.1021/nl503085v | Nano Lett. 2014, 14, 6010−6015

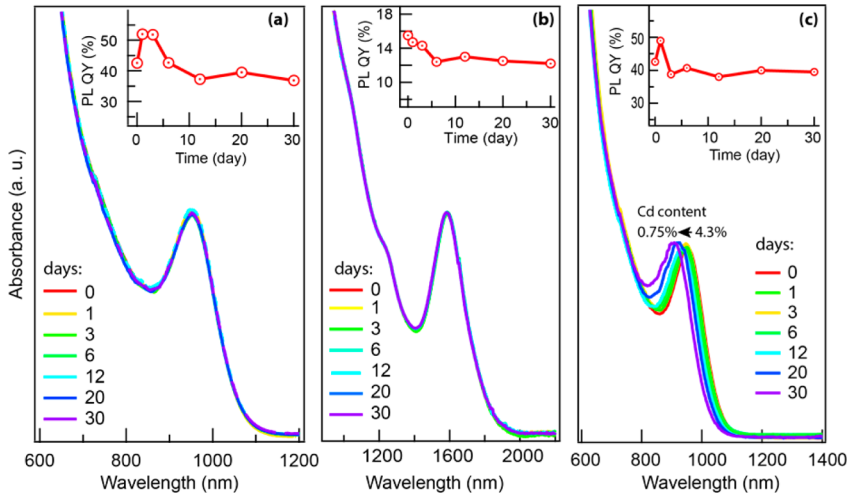

Figure 3. Temporal evolution of absorption spectra of hexane solutions of PbSe QDs with the first excitonic peak at 950 nm (a) and 1585 nm (b) stored in air. The insets display the corresponding PL QY as a function of time. (c) Absorption spectra of PbSe QDs stored in TCE for 30 days. The blue shift of the peak occurs due to Cd assisted surface etching of the PbSe QDs resulting in smaller QDs after 30 days. The content of residual Cd within the resulting QDs decreases to less than 1%.

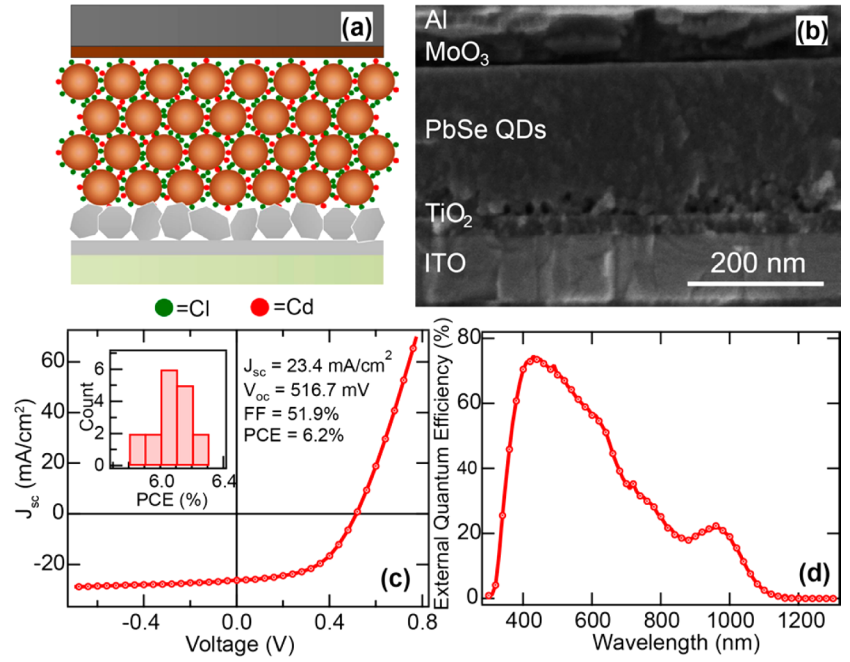

Figure 4. (a) A schematic solar cell structure and (b) a cross-sectional scanning electron microscopy image of the device. (c) The $J-V$ characteristics and (d) the EQE spectrum of a representative PbSe QD solar cell. Inset in c shows the histogram of device efficiencies obtained based on measurements of 17 solar cells.

prepared via a layer-by-layer dip coating in a fume hood. The ITO/TiO_2 substrate was hand-dipped into the PbSe QD solution in hexane (~10 mg/mL), slowly withdrawn, allowed to dry, and then dipped into the 1-mM EDT solution in acetonitrile. Twenty-five dip cycles were performed to build up a layer that is 260−280 nm thick (further details are provided in the Supporting Information).

The current−voltage ($J-V$) characteristics and the external quantum efficiency (EQE) spectrum of a representative device are displayed in Figure 4c and d. The device shows a short-circuit current (J_{SC}) of 23.4 mA/cm^2, an open-circuit voltage (V_{OC}) of 516.7 mV, a fill factor (FF) of 51.9%, and a power conversion efficiency (PCE) of 6.2%. Integrating the product of the AM1.5G photon flux and the EQE spectrum yields J_{SC} of 22.4 mA/cm^2, which is in a good agreement with the measurement. Our devices demonstrate excellent reproducibility. Out of 17 solar cells tested by us, more than 10 devices showed the PCE above 6% (inset of Figure 4c). Furthermore, they also show good stability. Specifically, the $J-V$ scans were periodically recorded every 24 h to characterize V_{OC}, J_{SC}, FF, and PCE. These measurements indicated that the devices were stable for at least 4 days. In a previous report we showed that air-stable solar cells could be also fabricated using PbSe QDs synthesized from $PbCl_2$. The efficiency of these devices of ~2.7%, however, was lower. They also exhibited a poorer stability and showed signs of degradation shortly after exposure to light.[24] In the present study, the PCE improvement is likely derived from two factors: reduced recombination losses due to

dx.doi.org/10.1021/nl503085v | Nano Lett. 2014, 14, 6010−6015

combination of Cl and Cd passivations and increased photovoltage due to the use of smaller QDs. A more complete passivation of QD surfaces is also a likely reason for the improved device stability.

In summary, we have reported a direct cation-exchange synthesis of PbSe QDs with a large range of sizes and in situ chloride and cadmium passivation. These QDs show high PL QYs that remain stable in air for more than 30 days. The characterization of the fabricated materials by HRTEM, XRD, and XPS indicates that the Cd and Cl ions reside on the QD surface rather than the QD interior. Furthermore, we demonstrate a prototype p−n junction solar cell made in air with a PCE of 6.2%, which is a record for PbSe QD -PVs. These results demonstrate that new synthetic strategies can lead to improved performance characteristics of PbSe QD-PVs that approach those of PbS QD-PVs with respect to both PCE and long-term stability under ambient conditions. We are currently applying these principles to develop high-efficiency, low band gap, air-stable PbSe QD-PV with enhanced MEG characteristics.

■ ASSOCIATED CONTENT

Supporting Information

Experimental details, absorption spectra of starting CdSe QDs, XPS data, and stability studies of PbSe QD solar cells. This material is available free of charge via the Internet at http://pubs.acs.org.

■ AUTHOR INFORMATION

Corresponding Author

*E-mail: matt.beard@nrel.gov.

Author Contributions

J.Z. and J.G. contributed equally to the present study.

Notes

The authors declare no competing financial interest.

■ ACKNOWLEDGMENTS

This material is based upon work supported by the U.S. Department of Energy Office of Science, Office of Basic Energy Sciences Energy Frontier Research Centers program within the Center for Advanced Solar Photophysics. DOE funding was provided to NREL through contract DE-AC36-08G028308. XPS work was conducted with support from an NREL Director's Postdoctoral Fellowship.

■ REFERENCES

(1) Semonin, O. E.; Luther, J. M.; Beard, M. C. Quantum dots for next-generation photovoltaics. *Mater. Today* **2012**, *15*, 508−515.

(2) Talapin, D. V.; Lee, J. S.; Kovalenko, M. V.; Shevchenko, E. V. Prospects of Colloidal Nanocrystals for Electronic and Optoelectronic Applications. *Chem. Rev.* **2010**, *110*, 389−458.

(3) Alivisatos, A. P. Semiconductor Clusters, Nanocrystals, and Quantum Dots. *Science* **1996**, *271*, 933−937.

(4) McGuire, J. A.; Joo, J.; Pietryga, J. M.; Schaller, R. D.; Klimov, V. I. New Aspects of Carrier Multiplication in Semiconductor Nanocrystals. *Acc. Chem. Res.* **2008**, *41*, 1810−1819.

(5) Shabaev, A.; Hellberg, C. S.; Efros, A. L. Efficiency of Multiexciton Generation in Colloidal Nanostructures. *Acc. Chem. Res.* **2013**, *46*, 1242−1251.

(6) Beard, M. C.; Luther, J. M.; Semonin, O. E.; Nozik, A. J. Third Generation Photovoltaics based on Multiple Exciton Generation in Quantum Confined Semiconductors. *Acc. Chem. Res.* **2013**, *46*, 1252−1260.

(7) Chuang, C.-H. M.; Brown, P. R.; Bulović, V.; Bawendi, M. G. Improved performance and stability in quantum dot solar cells through band alignment engineering. *Nat. Mater.* **2014**, *13*, 796−801.

(8) http://www.nrel.gov/ncpv/images/efficiency_chart.jpg (accessed September 2014).

(9) Luther, J. M.; et al. Stability Assessment on a 3% Bilayer PbS/ZnO Quantum Dot Heterojunction Solar Cell. *Adv. Mater.* **2010**, *22*, 3704−3707.

(10) Gao, J. B.; et al. n-Type Transition Metal Oxide as a Hole Extraction Layer in PbS Quantum Dot Solar Cells. *Nano Lett.* **2011**, *11*, 3263−3266.

(11) Shabaev, A.; Efros, A. L.; Efros, A. L. Dark and Photo-Conductivity in Ordered Array of Nanocrystals. *Nano Lett.* **2013**, *13*, 5454−5461.

(12) Ehrler, B.; et al. Preventing interfacial recombination in colloidal quantum dot solar cells by doping the metal oxide. *ACS Nano* **2013**, *7*, 4210−4220.

(13) McGuire, J. A.; Sykora, M.; Joo, J.; Pietryga, J. M.; Klimov, V. I. Apparent Versus True Carrier Multiplication Yields in Semiconductor Nanocrystals. *Nano Lett.* **2010**, *10*, 2049−2057.

(14) Beard, M. C.; et al. Comparing Multiple Exciton Generation in Quantum Dots To Impact Ionization in Bulk Semiconductors: Implications for Enhancement of Solar Energy Conversion. *Nano Lett.* **2010**, *10*, 3019−3027.

(15) Midgett, A. G.; et al. Size and Composition Dependent Multiple Exciton Generation Efficiency in PbS, PbSe, and PbSxSe1-x Alloyed Quantum Dots. *Nano Lett.* **2013**, *13*, 3078−3085.

(16) Semonin, O. E.; et al. Peak External Photocurrent Quantum Efficiency Exceeding 100% via MEG in a Quantum Dot Solar Cell. *Science* **2011**, *334*, 1530−1533.

(17) Talapin, D. V.; Murray, C. B. PbSe nanocrystal solids for n- and p-channel thin film field-effect transistors. *Science* **2005**, *310*, 86−89.

(18) Luther, J. M.; et al. Structural, optical and electrical properties of self-assembled films of PbSe nanocrystals treated with 1,2-ethanedithiol. *ACS Nano* **2008**, *2*, 271−280.

(19) Sykora, M.; et al. Effect of Air Exposure on Surface Properties, Electronic Structure, and Carrier Relaxation in PbSe Nanocrystals. *ACS Nano* **2010**, *4*, 2021−2034.

(20) Bae, W. K.; et al. Highly Effective Surface Passivation of PbSe Quantum Dots through Reaction with Molecular Chlorine. *J. Am. Chem. Soc.* **2012**, *134*, 20160−20168.

(21) Hughes, B. K.; et al. Control of PbSe Quantum Dot Surface Chemistry and Photophysics Using an Alkylselenide Ligand. *ACS Nano* **2012**, *6*, 5498−5506.

(22) Ip, A. H.; et al. Hybrid passivated colloidal quantum dot solids. *Nat. Nanotechnol.* **2012**, *7*, 577−582.

(23) Moreels, I.; et al. Size-Tunable, Bright, and Stable PbS Quantum Dots: A Surface Chemistry Study. *ACS Nano* **2011**, *5*, 2004−2012.

(24) Zhang, J.; Gao, J.; Miller, E. A.; Luther, J. M.; Beard, M. C. Diffusion Controlled Synthesis of PbS and PbSe Quantum Dots with In-Situ Halide Passivation for Quantum Dot Solar Cells. *ACS Nano* **2013**, *8*, 614−622.

(25) Woo, J. Y.; et al. Ultrastable PbSe Nanocrystal Quantum Dots via In Situ Formation of Atomically Thin Halide Adlayers on PbSe(100). *J. Am. Chem. Soc.* **2014**, *136*, 8883−8886.

(26) Thon, S. M.; et al. Role of Bond Adaptability in the Passivation of Colloidal Quantum Dot Solids. *ACS Nano* **2013**, *7*, 7680−7688.

(27) Voznyy, O.; Thon, S. M.; Ip, A. H.; Sargent, E. H. Dynamic Trap Formation and Elimination in Colloidal Quantum Dots. *J. Phys. Chem. Lett.* **2013**, *4*, 987−992.

(28) Fayette, M.; Robinson, R. D. Chemical transformations of nanomaterials for energy applications. *J. Mater. Chem. A* **2014**, *2*, 5965−5978.

(29) Hughes, B. K.; Luther, J. M.; Beard, M. C. The Subtle Chemistry of Colloidal, Quantum-Confined Semiconductor Nanostructures. *ACS Nano* **2012**, *6*, 4573−4579.

(30) Luther, J. M.; Zheng, H. M.; Sadtler, B.; Alivisatos, A. P. Synthesis of PbS Nanorods and Other Ionic Nanocrystals of Complex

Morphology by Sequential Cation Exchange Reactions. *J. Am. Chem. Soc.* **2009**, *131*, 16851−16857.
(31) Pietryga, J. M.; et al. Utilizing the lability of lead selenide to produce heterostructured nanocrystals with bright, stable infrared emission. *J. Am. Chem. Soc.* **2008**, *130*, 4879−4885.
(32) Neo, D. C. J.; et al. Influence of Shell Thickness and Surface Passivation on PbS/CdS core/shell Colloidal Quantum Dot Solar Cells. *Chem. Mater.* **2014**, *26*, 4004−4013.
(33) Pu, C. D.; et al. Highly reactive, flexible yet green Se precursor for metal selenide nanocrystals: Se-octadecene suspension (Se-SUS). *Nano Res.* **2013**, *6*, 652−670.
(34) Son, D. H.; Hughes, S. M.; Yin, Y. D.; Alivisatos, A. P. Cation exchange reactions -in ionic nanocrystals. *Science* **2004**, *306*, 1009−1012.
(35) Lee, S.; et al. Slow colloidal growth of PbSe nanocrystals for facile morphology and size control. *RSC Adv.* **2014**, *4*, 9842−9850.
(36) Beberwyck, B. J.; Surendranath, Y.; Alivisatos, A. P. Cation Exchange: A Versatile Tool for Nanomaterials Synthesis. *J. Phys. Chem. C* **2013**, *117*, 19759−19770.
(37) Gupta, S.; Kershaw, S. V.; Rogach, A. L. 25th Anniversary Article: Ion Exchange in Colloidal Nanocrystals. *Adv. Mater.* **2013**, *25*, 6923−6943.
(38) Ihly, R.; Tolentino, J.; Liu, Y.; Gibbs, M.; Law, M. The Photothermal Stability of PbS Quantum Dot Solids. *ACS Nano* **2011**, *5*, 8175−8186.
(39) Norris, D. J.; Efros, A. L.; Erwin, S. C. Doped nanocrystals. *Science* **2008**, *319*, 1776−1779.